Smart Structures and Systems, *Vol. 27*, *No. 2* (*2021*) *305-318*
DOI: https://doi.org/10.12989/sss.2021.27.2.305

Monitoring an iconic heritage structure with OMA: the Main Spire of the Milan Cathedral

Antonello Ruccolo [1a], Carmelo Gentile*[1] and Francesco Canali [2b]

[1] *Department of Architecture*, *Built Environment and Construction Engineering* (*DABC*), *Politecnico di Milano*, *Piazza Leonardo da Vinci*, *32*, *20133 Milan*, *Italy*
[2] *Veneranda Fabbrica del Duomo di Milano*, *Via Carlo Maria Martini*, *1*, *20122 Milan*, *Italy*

(*Received July 6*, *2020*, *Revised September 20*, *2020*, *Accepted November 4*, *2020*)

Abstract. One of the most remarkable structural elements characterizing the Milan Cathedral is its Main Spire, built in Candoglia marble and completed in 1769. The Main Spire, reaching the height of about 108 m and supporting the statue of the Virgin Mary, is about 40 m high and stands on the octagonal *tiburio* erected around the main dome. The structural arrangement of the spire includes a central column which is connected through a spiral staircase to 8 perimeter columns and each column is stiffened by inverse flying buttress. Metallic clamps and dowels connect the marble blocks and metallic rods connect the perimeter columns to the central core. A large monitoring system was recently installed in the Milan Cathedral, including seismometers and temperature sensors at 3 levels of the Main Spire as well as a weather station at the top of the spire. After a concise historic background on the Main Spire and the description of the sensing devices installed in this structure, the paper focuses on the dynamic characteristics of the spire and their evolution during a time span of about 16 months. The presented results highlight that: (a) a high density of vibration modes is automatically detected in the frequency range 1.0-7.0 Hz; (b) the lower identified modes correspond to global modes of the cathedral; (c) the normal evolution in time of the resonant frequencies is characterized by clear fluctuations induced by the environmental effects (temperature and wind); (d) especially the dependence of resonant frequencies on temperature is very distinctive and reveals the key role of the metallic elements in the overall dynamic behavior; (e) notwithstanding the remarkable effects exerted by the changing environment on the resonant frequencies, output-only removal of environmental effects and novelty analysis allow an effective monitoring of the structural condition.

Keywords: architectural heritage; automated modal identification; closely spaced modes; environmental effects; structural health monitoring

1. Introduction

The Milan Cathedral (Fig. 1) is a monumental cross-shaped church partly designed in Gothic style, whose structural construction took more than 4 centuries, from the beginning of apse erection in 1386 until the façade finalization in 1813 (Veneranda Fabbrica del Duomo 1885). Subsequently, the architectural works continued until the installation of the last iron gate in the façade – on January 6th, 1965 – that is usually indicated as the official completion of the building works. Far from being just the most representative landmark of the city of Milan, the Cathedral is one of the largest masonry monuments ever built, spreading over an area of more than 10400 m^2 and with a volume of about 300000 m^3.

One of the most iconic elements of the Milan Cathedral is its Main Spire (Nava 1848, Veneranda Fabbrica del Duomo 1885), consisting of a high octagonal structure – in pink-veined white marble from the Candoglia quarries – supported, at 65 m from the ground, by the main dome and the *tiburio* (i.e., the prismatic structure with octagonal base, which is built around the dome).

Since 1387, all the operational aspects related to the construction, maintenance and preservation of the Milan Cathedral are in charge of the historic Institution named *Veneranda Fabbrica del Duomo di Milano* (see e.g., Ferrari da Passano 1973), and denoted to as *Fabbrica* in the following. As the erection of the cathedral's main structures proceeded and was completed, the *Fabbrica* main mission moved to maintenance through the continuous inspection and architectural restoration of surfaces and statues in Candoglia marble. Besides the well-established time-based architectural maintenance program, the preservation of the structural integrity of the monument is hindered by the dimensions and the complexity of the building, as well as by the difficulty to reach and inspect several structural elements.

In order to enhance the efficiency of the structural inspections and early detecting the onset of potential anomalies and issues, a monitoring network (Gentile *et al*. 2019) has been designed and installed in the monument, with the two-fold objective of providing the information

*Corresponding author, Professor,
E-mail: carmelo.gentile@polimi.it
[a] Ph.D. Candidate, E-mail: antonello.ruccolo@polimi.it
[b] Technical Director, E-mail: dl.cantieri@duomomilano.it

http://www.techno-press.org/?journal=sss&subpage=7
ISSN: 1738-1584 (Print), 1738-1991 (Online)

(a) Past view (b) Present view

Fig. 1 Views of the Milan Cathedral (courtesy of *Veneranda Fabbrica del Duomo di Milano*)

needed for the condition-based structural maintenance and improving the knowledge of the building through the collection of a large archive of experimental data. It should be noticed that, unlike previous experiences of long-term monitoring large churches (see e.g., Potenza *et al*. 2015, Masciotta *et al*. 2016, Elyamani *et al*. 2017, Masciotta *et al*. 2017, Zonno *et al*. 2019), monumental buildings (Kita *et al*. 2019) and towers (Gentile *et al*. 2016, Cabboi *et al*. 2017b, Ubertini *et al*. 2018), where a limited number of sensing devices was used, the monitoring system implemented in the Milan Cathedral includes a relatively large number of sensors for measuring both static (15 bi-axial tilt-meters and 12 vibrating wire extensometers) and dynamic parameters (36 uni-axial seismometers); in addition, the indoor and outdoor environmental conditions are extensively monitored.

In designing the monitoring system of the Milan Cathedral (Gentile *et al*. 2019), utmost attention has been paid to the Main Spire (Fig. 2), which already underwent several restoration works (Nava 1845, Zacchi 1941), despite it is one of the youngest sub-structures of the cathedral. The dynamic characteristics of the Main Spire, a slender structure resting on the support provided by the *tiburio* and the main dome of the Milan Cathedral, are expected to be driven by the peculiar structural arrangement of the spire (Fig. 2); consequently, OMA of the cathedral (Gentile *et al*. 2019) and the spire, as well as the related vibration-based Structural Health Monitoring (SHM), should be independently performed.

In addition, previous studies on the dynamic characterization of historic slender structures (see Diaferio *et al*. 2018 for a list of recent studies on ancient towers) has motivated the installation of a dynamic monitoring system in the Main Spire: the modal parameters are extracted from the collected time series on a hourly basis, providing useful information on the structural performance.

The application of vibration-based SHM of slender historical structures has elected the natural frequencies as effective damage-sensitive features, apt to promptly identify the occurrence of structural anomalies (see e.g., Gentile *et al*. 2016, Ubertini *et al*. 2018). On the other hand, it is generally recognized that the environmental conditions also affect the natural frequencies, with undesired effects for SHM purposes. Therefore, a reliable novelty detection

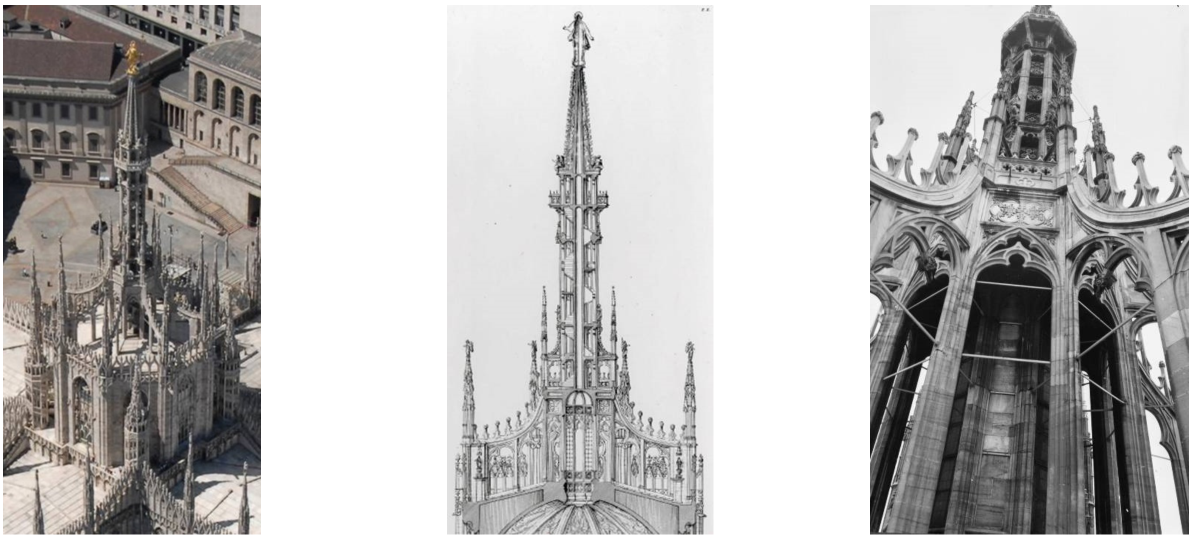

(a) View of the Main Spire (b) Historic drawing (c) Metallic rods connecting flying buttresses and columns

Fig. 2 Views of the Main Spire and *tiburio* of the Milan Cathedral (courtesy of *Veneranda Fabbrica del Duomo di Milano*) procedure based on natural frequencies should include the removal of environmental effects.

In this study, the SHM strategy comprises: (i) collection of vibration data from the sensors installed at 3 levels of the spire, (ii) estimation of natural frequencies via fully-automated Operational Modal Analysis (OMA, see e.g., Reynders *et al*. 2012), (iii) filtering out the environmental effects from the natural frequencies by means of Principal Component Analysis (PCA, Jolliffe 2002) and (iv) novelty analysis based on control charts fed by cleansed frequencies (Montgomery 1997).

The paper is subdivided as follows. A concise description of the Main Spire and its dynamic monitoring system is given in Section 2, along with an essential chronology of the spire construction and restoration works. Section 3 addresses the methodology implemented to automatically identify the natural frequencies and to exploit them for damage detection purposes. The dynamic characteristics of the spire are described in Section 4, whereas the evolution in time of natural frequencies is discussed in Section 5. After the peculiar influence of the environmental conditions on the identified natural frequencies is presented and discussed, the removal of environmental effects and the novelty analysis strategy are exemplified in Section 6.

2. The Main Spire of the Milan Cathedral and its monitoring system

The Main Spire is a slender structure supporting the statue of the Virgin Mary – known as *Madonnina* in Italy – at a height of 108.5 m from the ground, above the major altar. The devotion of the city towards this statue is such that local laws have prevented for centuries any other building erected in Milan from exceeding the height of the *Madonnina*; even nowadays, reproductions of the statue are placed on the top of the tallest skyscrapers of Milan.

2.1 Description of the Main Spire

Similarly to the entire Milan Cathedral, the Main Spire (Figs. 2 and 3) is a complex system in which Candoglia marble, masonry and metallic elements are arranged together and collaborate to provide the structure with the required stiffness and strength (see e.g., Nava 1845). The structure of the spire can be ideally subdivided into 3 main parts (Zacchi 1941):

- The base, about 9.0 m high, ranging from the top of the *tiburio* to the lower Belvedere. In this part, 8 inverse flying arches connect the 8 perimeter columns of the spire to the load-bearing walls of the octagonal *tiburio* (Figs. 2(a)-(c)), so that the lateral thrust induced by wind gusts is conveyed to the *tiburio*. The resisting mechanism is completed by the metallic tie-rods placed at the base of the flying buttresses, as shown in Fig. 2(c);
- The central core, about 19.4 m high, consisting of a hollow cylindrical pier surrounded by eight minor columns (Fig. 3). The perimeter columns are linked together by ornamental elements, whereas the connection between the main pier and the perimeter columns is provided by a spiral staircase (Fig. 3(a)), that allows reaching the upper Belvedere, rising at 91.7 m from the ground;
- The pinnacle, 14.8 m high, on the top of which is lodged the *Madonnina* (Figs. 2(a)-(b)).

The Main Spire can thus be assumed as a 45 m long vertical cantilever, resting on the main dome at 65 m from the ground. It is further noticed that the structural arrangement of the spire includes: (a) several clamps connecting the adjacent marble blocks, (b) large metallic rods connecting the eight perimeter columns and the central core (Figs. 2(c) and 3(b)), and (c) C shaped flat-rolled profiles running across the overall height of the central column (Fig. 3(a)), providing both bending reinforcement and lateral confinement.

It should be stressed that most of metallic elements of the Main Spire dates back to the original design (even if tie-rods, metallic clamps and dowels have been replaced during various maintenance/strengthening interventions). As a matter of fact, it is stated in (Nava 1845) that “the Main Spire can be modeled as a metallic frame, balanced by concentric vertical forces, disguised and resting on a marble

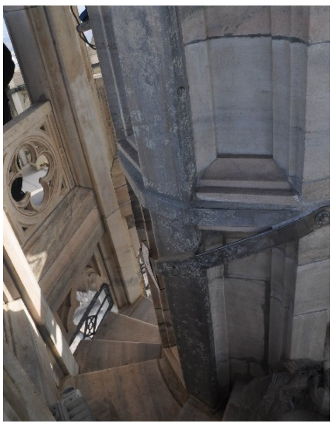

(a) Vertical and helicoidal profiles

(b) Concentric profiles and radial rods

Fig. 3 Details of the Main Spire metallic reinforcements cladding, which constitutes the exterior shape of the artifact".

A brief chronology of the Main Spire, including the main interventions, follows:

- 1762, Architect Francesco Croce is appointed to design the structure;
- 1765-1769, the Main Spire is erected;
- January 1842, visual inspections revealed a poor state of conservation of several marble blocks and spread corrosion of the metallic rods. The resolution of the Architect Pietro Pestagalli to tear down the structure and build it ex-novo was successfully opposed by Count Ambrogio Nava, who proposed a restoration project;
- 1844-1845, restoration works are directed by Count Ambrogio Nava (Nava 1845);
- 1902, after a series of inspections required by the *Fabbrica*, a team of specialists and technicians highlighted the poor structural condition of the Main Spire but safety issues were excluded. Subsequently, maintenance works on the spire and its flying arches were carried out;
- 1904, an inverted pendulum was installed in the structure to measure the horizontal deformation induced by strong winds (Vicentini 1906);
- 1941, restoration works under the direction of Architect Adolfo Zacchi;
- 1967, Architect Carlo Ferrari da Passano proceeded with a scrupulous substitution of selected iron ties in the spire with elements in stainless steel. In addition, vertical radial and helicoidal confinement of the central core has been improved (Fig. 3);
- 2010, the last restoration works are performed to substitute degraded marble blocks. During this intervention, wire extensometers were used to survey the interaction between the Main Spire and the surrounding scaffolding (Cigada *et al*. 2020).

2.2 Description of the monitoring system

The dynamic monitoring system installed in the Milan Cathedral (Gentile *et al*. 2019) and in the Main Spire is based on SARA SS45 seismometers (electro-dynamic velocity sensors). It should be noticed that seismometers exhibit high sensitivity of 78 V/(m/s), un-necessity of powering and excellent performance in the low frequency range ($f \leq 100$ Hz), so that those transducers turn out to be especially suitable for the application in vibration testing (Roselli *et al*. 2018) and/or monitoring (Azzara *et al*. 2018) of civil engineering and cultural heritage structures. In addition, the seismometers offer the possibility of estimating the displacement time series by integrating the velocity signals, so that data directly related to the stiffness

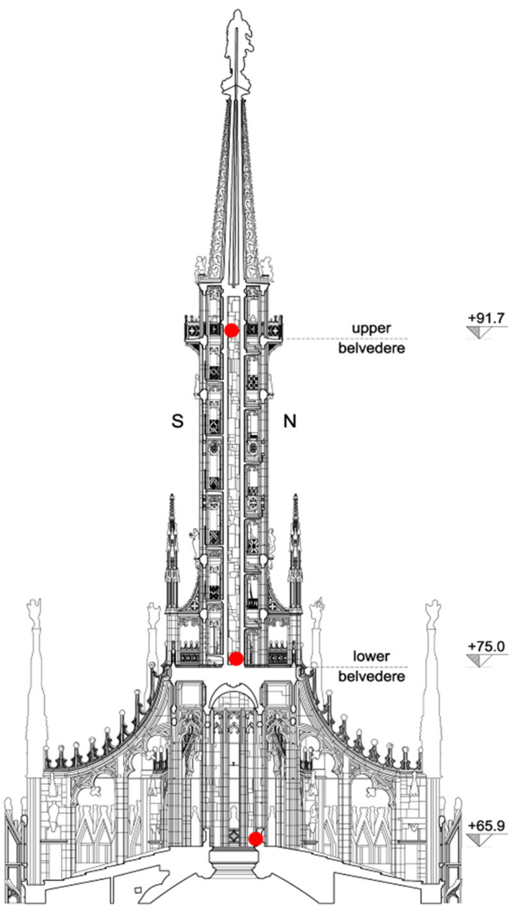

(a) Sensors layout (elevation)

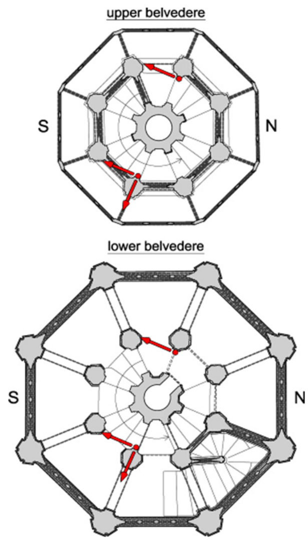

(b) Sensors layout (plan)

(c) Seismometer on site

Fig. 4 Dynamic monitoring system installed in the Main Spire (and especially useful for the slender Main Spire) are conceivably available.

9 seismometers are installed at 3 levels of the Main Spire, according to the layout exemplified in Fig. 4: (a) 1 tri-axial seismometer is placed at the base of the spire (+65.9 m); (b) 3+3 horizontal uni-axial seismometers are mounted at the level of lower Belvedere (+75.0 m) and upper Belvedere (+91.7 m), respectively. The 3+3 sensors installed in the lower and upper Belvedere are mounted on two opposite perimeter columns of the spire (Fig. 4). Each sensors triad is wired to one 24-bit digitizer, with the digitizers being connected to a switch for data transfer.

The Main Spire also hosts static measurement devices: 3 couples of tilt-meters (measuring the static rotation in the North-South and East-West directions), temperature sensors integrated with each tilt-meter and one weather station installed on the higher accessible level.

It worth mentioning that the dynamic monitoring of the Milan Cathedral is fully active since mid October 2018 (Gentile *et al*. 2019); on the other hand, the seismometers were mounted in the Main Spire at the beginning of June 2018, so that preliminary OMA has been conducted for several weeks since June 6th, 2018.

3. SHM methodology: from data processing to novelty detection

The vibration-based SHM methodology adopted for the Main Spire is based on a multi-level procedure developed in the Matlab framework and involving the following steps (Fig. 5):

- preliminary pre-processing of the raw data;
- automated OMA and estimation of natural frequencies;
- removal of environmental effects from the natural frequencies;
- novelty detection.

The pre-processing of the measured velocities comprises the following tasks: (a) de-convolution of the raw data (to compensate the low-frequency attenuation of the sensors) and subsequent saving into a Matlab-compatible format; (b) de-trending, de-spiking and evaluation of the maximum and root mean square value of each time series; (c) low-pass filtering applying a 7th order Butterworth filter and 5th order decimation of data, reducing the sampling frequency from 100 Hz to 20 Hz. At the end of this preliminary stage, a new file (containing 9×20 samples/s × 3600 s/hour = 648000 velocity values) is stored, each hour, in a compact database.

The modal parameters of the Main Spire are identified using a fully automated procedure, based on the covariance-driven Stochastic Subspace Identification (SSI-Cov) algorithm (see e.g., Peeters and De Roeck 1999) and developed in previous studies (Cabboi 2013, Cabboi *et al*. 2017a). The length of the time window adopted in the automated identification was set equal to 1 h (3600 s). The adopted automated procedure involves the two main steps of modal parameters estimation (MPE) and modal tracking (MT).

The MPE is performed through an automatic interpretation of the stabilization diagram, based on the sensitivity of frequency and mode shape to the model order variation. For each dataset, after having filtered the spurious poles by checking the associated damping ratio and mode complexity value (Pappa *et al*. 1992, Heylen *et al*. 2007), the poles sharing similar frequencies and mode shapes are clustered together, and a set of representative modal parameters (i.e., resonant frequency, damping and mode shape) is estimated for each cluster. It is worth mentioning that the mode complexity is checked by averaging the information provided by both the Modal Phase Collinearity (MPC, Pappa *et al*. 1992) and Mean Phase Deviation (MPD, Pappa *et al*. 1992, Heylen *et al*. 2007) through the Modal Complexity Index (MCI = 0.5 × [(1 − MPC) + (MPD/45°)], varying between 0 and 1, with 0 indicating a mono-phase behavior of the identified mode shape).

In the MT, aimed at providing the time evolution of the parameters of each mode, the dynamic characteristics identified from each 1-h dataset are compared to a pre-selected list of reference modes in order to establish the right correspondence: the tracking of the structural modes is performed in terms of natural frequencies and mode shapes in an adaptive way. The interested reader is referred to (Cabboi 2013, Cabboi *et al*. 2017a) for additional details.

It is further noticed that: (a) 8 channels of horizontal velocity data are used in the automated OMA; (b) the time lag parameter i was set equal to 70 and the data were fitted using stochastic subspace models of order varying between 20 and 160; (c) in the noise modes elimination step, the maximum allowable damping ratio and MCI were set equal to 6% and 0.20, respectively.

As widely reported in the literature, the natural frequencies of structures and historic buildings also depend on the environmental and operational conditions, whose effects should be addressed and removed. In the present study, after the correlation between environmental/

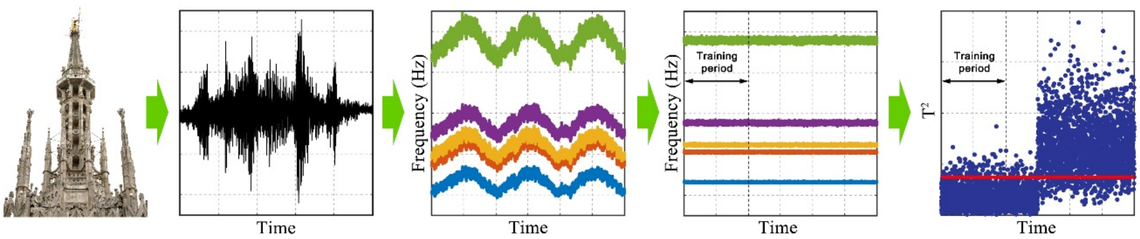

Fig. 5 Schematic of the SHM methodology adopted for the Main Spire of the Milan Cathedral

operational changes and natural frequencies has been highlighted, the Principal Component Analysis (PCA, Jolliffe 2002, Deraemaeker *et al*. 2008, Cabboi *et al*. 2017b, Azzara *et al*. 2018) is applied to remove the variance of natural frequencies that is associated to environmental/ operational factors.

Linear PCA models project the matrix containing N samples of n identified frequencies – $\mathbf{Y}\in\Re^{n\times N}$ – into a set of principal scores $\mathbf{X}\in\Re^{m\times N}$, according to the formula $\mathbf{X}=\mathbf{TY}$, where $\mathbf{T}\in\Re^{m\times n}$ is the loading matrix. The redundancy of information due to the correlation among the identified frequencies is thus exploited retaining only a reduced number of principal scores, $m < n$, which explain most of the variance of the identified frequencies. A set of predicted natural frequencies $\mathbf{Y}^*\in\Re^{n\times N}$ is estimated retaining only few principal components. As it will discussed in Section 6, in the case of the Main Spire of Milan Cathedral, a PCA-based regression model has been calibrated using the frequency estimates collected in a training period corresponding to the first year of monitoring: in the regression model, m = 4 principal components (out of 9 natural frequencies) have been retained in order to filter out the environmental/operational effects.

As long as no alteration occurs to the monitored structure, the established PCA model (i.e., the matrix **T** associated to the training period) is capable to predict the evolution of the newly identified natural frequencies. The prediction errors or residuals – i.e., the discrepancy between the identified natural frequencies and the predicted ones – represent a set of features only depending on the structural conditions and fully suitable to SHM. In order to promptly detect and magnify the occurrence of any anomalous pattern in the prediction errors, conceivably induced by structural changes or damages, the SHM strategy is finalized with a control chart, such as the Hotelling's T^2 distance (Montgomery 1997). As any structural anomaly occurs, the statistical properties of the residuals would exhibit a sudden change and the T^2 values would systematically exceed a threshold limit (Fig. 5, Magalhães 2010).

4. Dynamic characteristics of the Main Spire

As previously pointed out, the dynamic characteristics

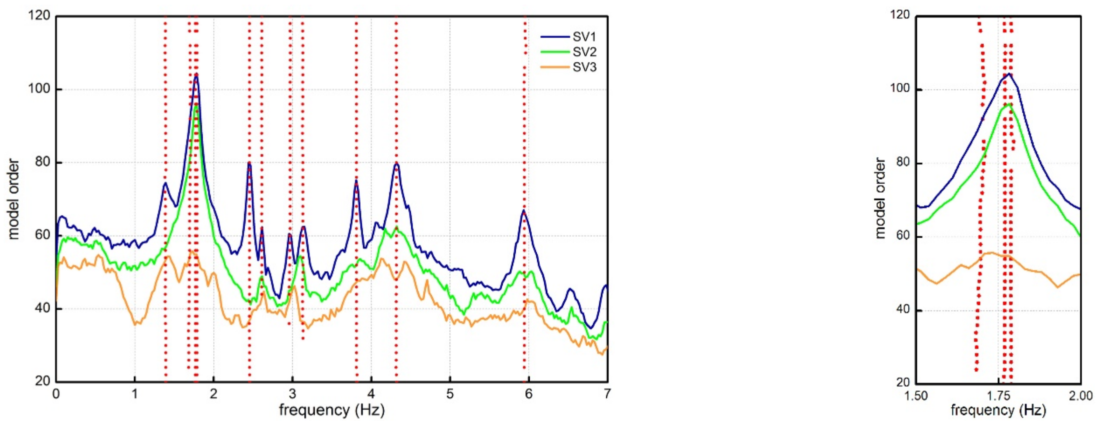

(a) Natural frequencies estimation via stabilization diagram (b) Zoom 1.5-2.0 Hz

Fig. 6 Application of the SSI-Cov technique to signals collected in the Main Spire of Milan Cathedral (8 channels of velocity data, June 6th, 2018, h 18:00-19:00)

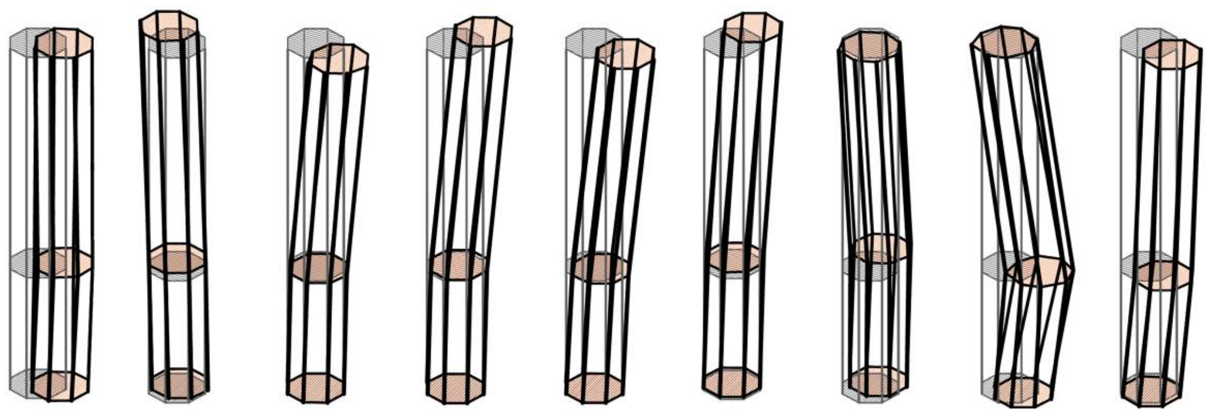

f= 1.39 Hz (a) C1 | f= 1.70 Hz (b) C2 | f= 1.77 Hz (c) S1 | f= 1.79 Hz (d) S2 | f= 2.45 Hz (e) S3 | f= 2.61 Hz (f) S4 | f= 2.97 Hz (g) S5 | f= 3.13 Hz (h) S6 | f= 3.81 Hz (j) S7

Fig. 7 Selected vibration modes of the Main Spire (SSI-Cov, June 6th, 2018, h 18:00-19:00) of the Main Spire have been evaluated since June 6th, 2018 and afterwards adopted as reference values during the continuous dynamic monitoring, that started on October 16th, 2018.

As shown in the stabilization diagram of Fig. 6(a), a high density of normal modes is detected in the frequency range 1-7 Hz, with three closely-spaced modes being clearly identified in about 0.1 Hz (Fig. 6(b)); the dynamic characteristics of the Main Spire are reported in Table 1 in terms of natural frequencies and damping ratios, whereas the corresponding mode shapes of selected vibration modes are shown in Fig 7.

The inspection of Fig. 7 firstly reveals that the lower two modes, C1 (Fig. 7(a)) and C2 (Fig. 7(b)), are characterized by natural frequencies of 1.39 and 1.70 Hz, respectively, and correspond to global modes of the Cathedral (Gentile *et al*. 2019). Mode C1 (Fig. 7(a)) is characterized by equal modal deflection of the base, lower and upper Belvedere; the deflections occur in the North-South direction and correspond to the global sway mode of the cathedral in that direction. Mode C2 (Fig. 7(b)) involves a roto-translation of the spire in the East-West direction, again complying with a global sway motion of the cathedral. It is further noticed that the damping ratios of modes C1 and C2 (Table 1) are remarkably higher than those of the local modes S1-S9 of the spire.

Table 1 Dynamic characteristics of the Main Spire estimated via SSI-Cov (06/06/2018, h 18:00-19:00)

Mode Id.	*f* (Hz)	ζ (%)	Mode Id.	*f* (Hz)	ζ (%)
C1	1.386	3.69	S5	2.966	1.09
C2	1.699	4.26	S6	3.128	1.28
S1	1.770	1.56	S7	3.811	0.74
S2	1.790	1.15	S8	4.318	1.16
S3	2.454	0.60	S9	5.937	1.12
S4	2.610	0.41	–	–	–

It is worth mentioning that only the frequencies of local modes S1-S9 will be used in a SHM perspective.

The sequence of the spire local modes includes:

(a) a couple of closely-spaced modes, S1 and S2, which are characterized by natural frequency of 1.77 and 1.79 Hz, respectively. Modes S1 (Fig. 7(c)) and S2 (Fig. 7(d)) involve bending in two orthogonal planes, corresponding to principal directions of the octagonal cross-section of the spire. The corresponding damping ratios are equal to 1.56% and 1.15%, respectively;
(b) a second couple of modes, S3 (Fig. 7(e)) and S4 (Fig. 7(f)), which are again characterized by bending of the spire in two orthogonal planes, corresponding to principal directions of the spire and different from the bending planes of S1 and S2. Modes S3 and S4 exhibit natural frequencies of 2.45 and 2.61 Hz, respectively;
(c) a subsequent couple of modes, S5 (Fig. 7(g)) and S6 (Fig. 7(h)), involve higher order bending of the spire and, unlike modes S1-S4, horizontal deflection of the base of spire. Modes S5 and S6 are characterized by frequencies equal to 3.03 and 3.23 Hz and damping ratios of 1.09 and 1.29%, respectively;
(d) mode S7 (Fig. 7(j)), exhibiting higher order bending in the NE-SW direction. The corresponding natural frequency is 3.81 Hz and the modal displacement of the lower and upper Belvedere are comparable in direction and amplitude;
(e) finally, a couple of torsion modes S8 and S9 is identified at 4.46 and 6.26 Hz. It should be noticed that lower and upper Belvedere exhibits in phase rotation for mode S8, whereas the rotations are in opposition of phase for mode S9.

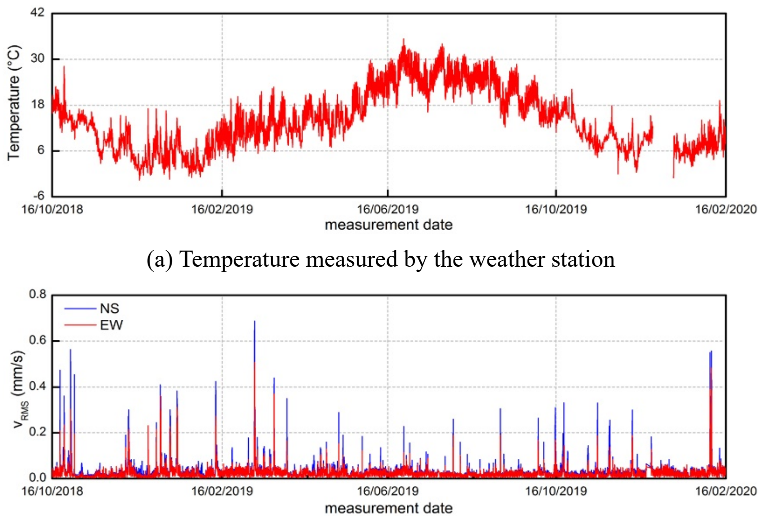

(a) Temperature measured by the weather station

(b) Hourly r.m.s. values of the velocity measured in the upper Belvedere

Fig. 8 Environmental parameters of the Main Spire

Table 2 Correlation coefficients among outdoor temperatures collected from 16/10/2018 to 15/10/2019

	T_1	T_2	T_3	T_{WS}
T_1	1.000	0.995	0.981	0.986
T_2	–	1.000	0.991	0.984
T_3	–	–	1.000	0.971
T_{WS}	–	–	–	1.000

5. Evolution of natural frequencies and effects of changing environment

5.1 Monitoring of the environmental parameters

SHM projects are usually complemented by the measurement of environmental parameters that might affect the structural response. As stated in sub-section 2.2, the dynamic monitoring of the Main Spire is assisted by 3 couples of temperature sensors installed along the height of the spire, as well as by a weather station placed in the upper Belvedere, so that a quite comprehensive description of the environmental conditions is attained.

It should be noticed that the temperature data (T_1, T_2 and T_3) measured at the three levels of the spire and by the weather station (T_{WS}) are highly correlated, as displayed in Table 2, so that only the temperature measured by the weather station, shown in Fig 8(a), is adopted for SHM purposes.

Due to the slenderness and the height of Main Spire, the amplitude of horizontal response exhibits good correlation with the wind speed and also accounts for other sources of excitation (such as subway transits, maintenance activities on the Cathedral roof, far-field earthquakes, etc). Hence, the root mean square of the signals collected on the upper Belvedere has been considered as an indirect measure of the level of dynamic excitation of the Main Spire. Fig. 8(b) shows the root mean square (r.m.s.) velocity in the N-S and the E-W directions, respectively: daily fluctuations of the vibration level are conceivably induced by the subway transits, maintenance works and other ambient excitations, whereas the r.m.s. peaks exceeding 0.2 mm/s reveal the presence of strong wind. It is worth mentioning that the r.m.s. values are estimated using the velocity data hourly measured.

5.2 Time evolution of natural frequencies

The results of the first 16 months of dynamic monitoring of the Main Spire – from October 16th, 2018 to February 15th, 2020 – are summarized and discussed in this section. More than 11000 1-h velocity datasets have been collected and automatically processed to extract the modal parameters and track their evolution in time. The time histories of the natural frequencies associated to local modes of the spire (S1-S9) are illustrated in Fig. 9, whereas Table 3 reports the statistical characterization in terms of mean value (f_{ave}), standard deviation (σ_f), maximum (f_{max})

Table 3 Statistics of identified natural frequencies from October 16th, 2018 to February 15th, 2020

Mode Id.	f_{ave} (Hz)	σ_f (Hz)	f_{min} (Hz)	f_{max} (Hz)	Id. rate (%)
S1	1.823	0.054	1.675	1.952	94.5
S2	1.845	0.055	1.705	1.994	95.9
S3	2.465	0.012	2.395	2.532	98.5
S4	2.614	0.016	2.534	2.688	81.0
S5	2.976	0.073	2.766	3.149	56.1
S6	3.220	0.064	2.978	3.355	75.3
S7	3.895	0.076	3.646	4.042	99.4
S8	4.435	0.095	4.213	4.744	99.3
S9	6.238	0.178	5.705	6.793	91.3

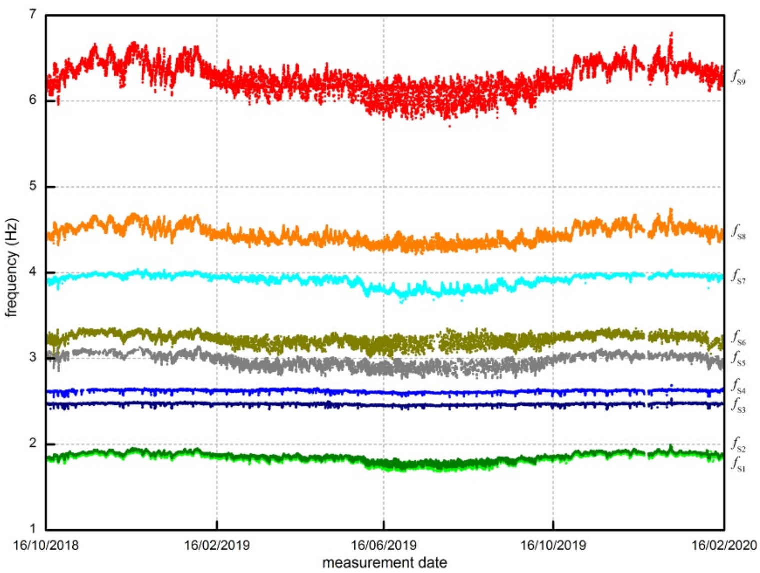

Fig. 9 Time evolution of the natural frequencies from October 16th, 2018 to February 15th, 2020

and minimum (f_{min}) values, and identification rate. Based on the inspection of Figs. 8(a) and 9, the following comments can be drawn:

(a) The level of ambient excitation allows the identification and tracking of 9 local modes in the range 1-7 Hz with high occurrence;
(b) The identification rate is higher for modes S1-S3 and S7-S9, ranging from 91.3% for S9 to 99.4% for S7, whereas it decreases to 56.1% for mode S5;
(c) All identified frequencies seem to evolve in time according to regular patterns mainly driven by the temperature and tend to increase with decreased temperature, with this distinctive trend being especially clear for modes S1-S2 and S5-S9;
(d) The negative dependence of natural frequencies on temperature is a distinctive behavior of the Main Spire and of the Milan Cathedral (Gentile *et al*. 2019), with this trend being very different from what generally reported in the long-term studies on masonry structures, either towers (Gentile *et al*. 2016, Cabboi *et al*. 2017b, Ubertini *et al*. 2018, Azzara *et al*. 2018) or churches (Masciotta *et al*. 2016, Elyamani *et al*. 2017, Masciotta *et al*. 2017).

Table 4 summarizes the correlation coefficients between the different natural frequencies in the investigated time span and highlights that the identified frequencies are characterized by correlation coefficients generally higher than 0.6, with the exception of the frequencies of modes S5-

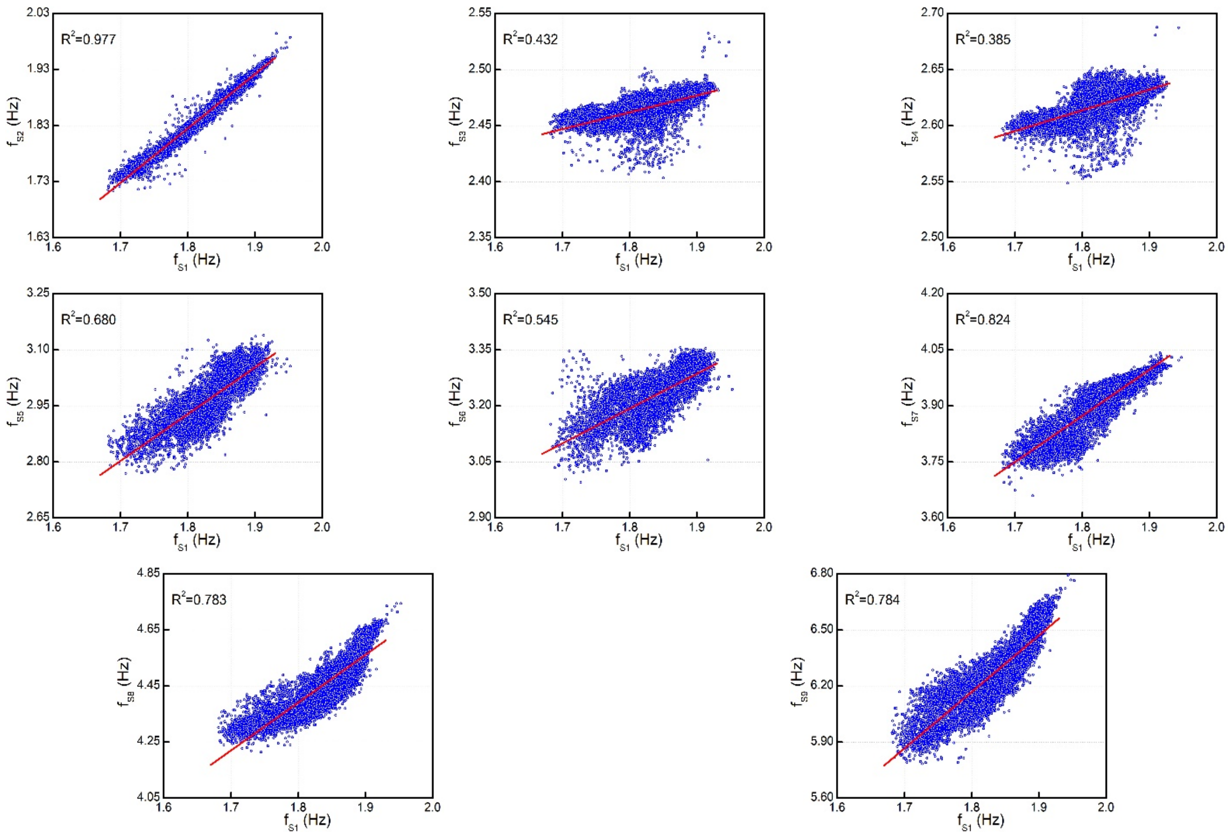

Fig. 10 Correlation between the natural frequency of modes S2-S9 and the frequency f_{S1}

Table 4 Correlation coefficients between the natural frequencies (from 16/10/2018 to 15/02/2020)

	f_{S1}	f_{S2}	f_{S3}	f_{S4}	f_{S5}	f_{S6}	f_{S7}	f_{S8}	f_{S9}
f_{S1}	1	0.952	0.642	0.590	0.752	0.688	0.871	0.875	0.867
f_{S2}	–	1	0.666	0.614	0.763	0.698	0.916	0.909	0.908
f_{S3}	–	–	1	0.892	0.443	0.346	0.720	0.660	0.604
f_{S4}	–	–	–	1	0.305	0.239	0.705	0.535	0.518
f_{S5}	–	–	–	–	1	0.821	0.626	0.729	0.725
f_{S6}	–	–	–	–	–	1	0.493	0.682	0.717
f_{S7}	–	–	–	–	–	–	1	0.849	0.818
f_{S8}	–	–	–	–	–	–	–	1	0.946
f_{S9}	–	–	–	–	–	–	–	–	1

S6, which are less correlated with the others. Moreover, closely spaced frequencies (i.e., f_{S1} and f_{S2}, f_{S3} and f_{S4}, f_{S5} and f_{S6}) exhibit correlation coefficients larger than 0.8. Similar comments can be drawn through the analysis of Fig 10, where the frequency of modes S2-S9 is plotted vs. the natural frequency f_{S1}, along with the regression line and the coefficient of determination R^2.

As previously stated (Fig. 9), the time evolution of the natural frequencies of the Main Spire reveals peculiar behavior. As exemplified in Fig. 11 with reference to f_{S2}, some natural frequencies exhibit inverse dependency with respect to the seasonal temperature (Figs. 11(a)-(b)), whereas the same frequencies increase with increased temperature on a daily base, as it is exemplified in Fig. 11(c) with reference to an interval of 10 days. Such a dual dependency is conceivably driven by the effects exerted by the different materials that constitute the Main Spire. In more details, the thermal expansion of the Candoglia marble induces the closure of micro-cracks with increased temperature, leading to a stiffening of the spire and to the daily increase of the natural frequencies. Conversely, the increase of seasonal temperature results in

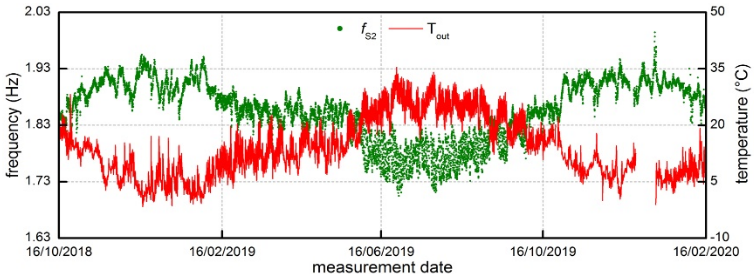

(a) Evolution in time of frequency f_{S2} and outer temperature

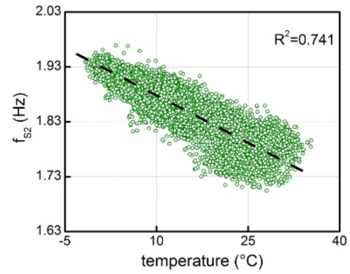

(b) Correlation between f_{S2} and T

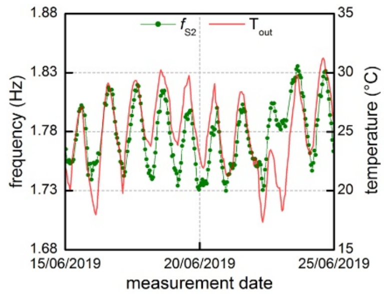

(c) Zoom of daily variations of f_{S2} and T

Fig. 11 Temperature effects on natural frequency f_{S2}

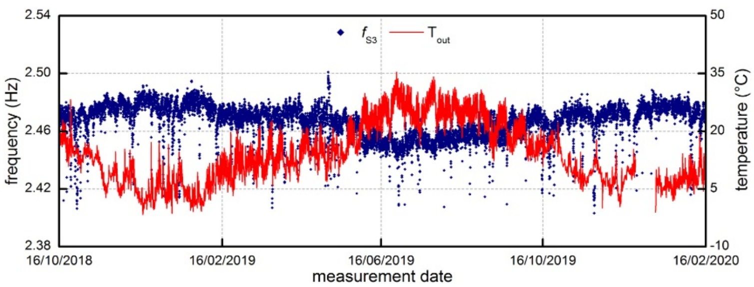

(a) Evolution in time of frequency f_{S3} and outer temperature

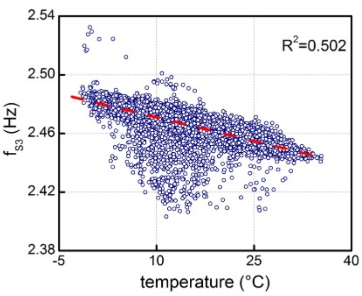

(b) Correlation between f_{S3} and T

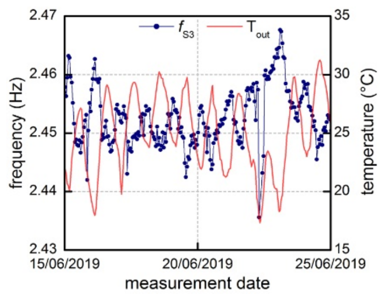

(c) Zoom of daily variations of f_{S3} and T

Fig. 12 Temperature effects on natural frequency f_{S3}

a slackening of the metallic confinement of the spire, leading to a global loss of stiffness and therefore to an overall decrease in the natural frequencies. The superposition of these two temperature-driven opponent effects conceivably explains the distinctive behavior of the frequency f_{S2}. It is worth mentioning that a similar complex dependence on temperature is observed for modes S1 and S5-S6 as well, whereas the frequency of higher (torsion) modes S8-S9 continues to exhibit an overall negative dependence on temperature but the daily effects are less clear.

Other natural frequencies (namely, the ones of modes S3-S4 and S7) exhibit a simpler correlation with the air temperature, as exemplified in Fig. 12 for f_{S3}: both seasonal and daily variations of frequency and temperature are in phase opposition. Hence, the evolution of mode S3 seems to be conceivably driven by the stiffening effect exerted by decreasing temperature on the metallic elements of the spire.

In addition to the influence of temperature, it should be remarked that the excitation associated to wind gusts induce temporary drops of natural frequencies f_{S3} and f_{S4} (Figs. 9 and 10). The typical correlation between frequency drops of f_{S3}, f_{S4} and the r.m.s. velocity (representing an indirect measure of the excitation level) is shown in Fig. 13 during a period of 10 days characterized by limited variations of the air temperature.

The temporary drops of natural frequencies f_{S3} and f_{S4}, corresponding to the increase of the response/excitation level (Fig. 13), suggest the occurrence of slightly non-linear behavior of the Main Spire induced by the increase of the horizontal forces associated to wind gusts.

6. Novelty analysis through principal component analysis and control charts

The damage detection methodology adopted for the Main Spire of the Milan Cathedral is finally exemplified in the present Section. As previously stated (Section 3), the SHM procedure is based on the analysis of the automatically identified natural frequencies and follows the steps schematically shown in Fig. 5, mainly involving the removal of frequency fluctuations driven by the environmental/operational effects and the subsequent application of novelty analysis.

Notwithstanding the complex dependence of natural frequencies on temperature, the approximately linear correlation (Fig. 10) observed among the identified natural frequencies suggests the application of output-only methods, such as the PCA-based regression (Jolliffe 2002), to remove the masking effects associated to varying environmental/operational conditions.

The calibration of a PCA-based regression requires the analysis of the covariance matrix of natural frequencies collected over a training period, covering a statistically representative sample of environmental/operational conditions; in the present application, the first year of monitoring (i.e., from 16/10/2018 to 15/10/2019) was assumed as training period. Once the singular values of the covariance matrix are computed and compared, the selection of the Principal Scores to retain depends on the cumulative percentage of variance explained by the first singular values. Fig. 14 shows the singular values of the covariance matrix of the 9 natural frequencies: it should be remarked that only one principal component is associated to more than 72% of data variance, due to the strong linear correlation among all frequencies (Fig. 10 and Table 4). The PCA model for regression and prediction of the natural frequencies of the Main Spire retains 4 principal components, accounting for more than 95% of the data variance.

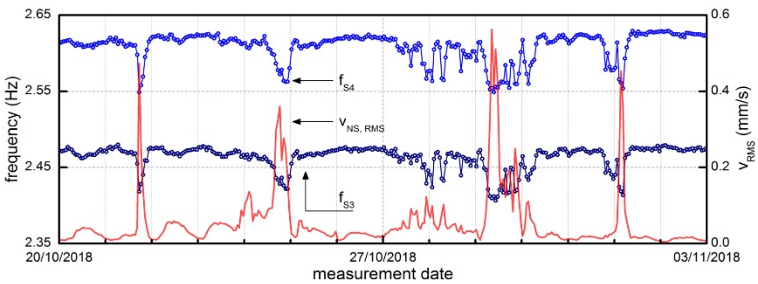

Fig. 13 Wind effects on frequencies f_{S3} and f_{S4}

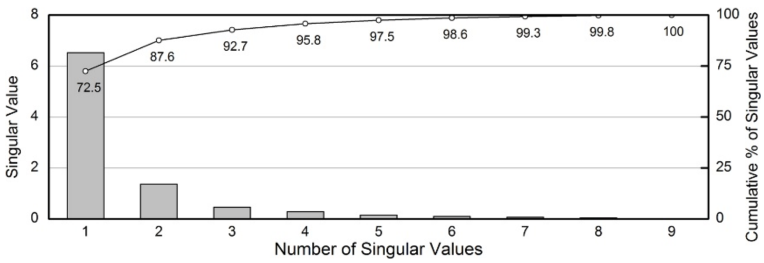

Fig. 14 Singular values of covariance matrix of natural frequencies (bars) and sum (lines)

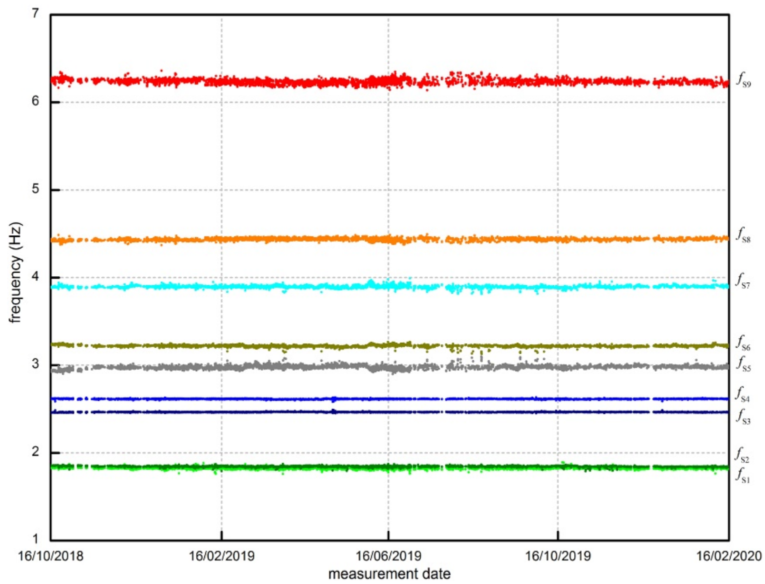

Fig. 15 Time evolution of the cleansed natural frequencies (4 principal components retained) from October 16th, 2018 to February 15th, 2020

After the PCA-based regression model has been established, it applies to new observations so that each set of hourly-estimated natural frequencies undergoes PCA regression and leads to a new set of predicted natural frequencies. The residuals (defined as the differences between identified and predicted natural frequencies) are expected to be insensitive to the factors modeled by the principal components until any structural change occurs. Fig. 15 shows the evolution in time of the cleansed natural frequencies (i.e., the sum of the average values during the training period and the residuals): the comparison between Figs. 9 and 15 provides evidence of the effectiveness of the PCA model in removing the environmental effect even after the training period (16/10/2018-15/10/2019).

The subsequent novelty analysis, performed by using the residuals, is finalized through the Hotelling's T^2 control chart (Montgomery 1997) with subgroups of 24 hours. According to this control chart, the statistical properties of each newly acquired subgroup of residuals are compared to the values identified during the training period. As long as the time evolution of T^2 remains below an upper control limit (UCL), the process is in control; conversely, if the UCL is systematically exceeded, the occurrence of structural anomaly is detected.

The time evolution of T^2 in the investigated monitoring period is shown in Fig. 16 and reveals limited variations, with only few outliers being detected out of the UCL (i.e., the dashed horizontal red line) after the end of the training period.

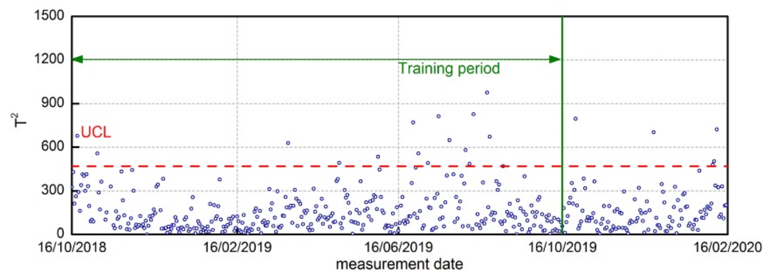

Fig. 16 Hotelling's T^2 control chart obtained for the Main Spire of the Milan Cathedral

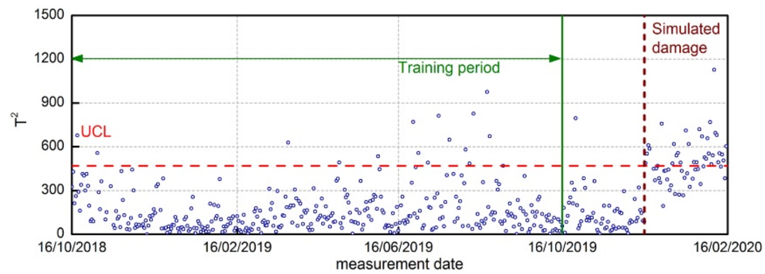

Fig. 17 Hotelling's T^2 control chart obtained by simulating slight frequency shifts

Finally, the sensitivity of the novelty analysis to slight damage in the structure has been investigated by simulating the occurrence of small frequency shifts (Gentile *et al*. 2016, Ubertini *et al*. 2018, Azzara *et al*. 2018) in the identified data. More specifically, small damages have been simulated by applying a shift in the values of the frequencies f_{S2} and f_{S4} − both involving bending in close directions − equal to 0.009 and 0.013 Hz, respectively. It should be pointed out that this damage scenario is relatively small when compared to the frequency shifts reported in the literature as induced by structural damages, that are undetectable by visual inspection (Gentile *et al*. 2016, Ubertini *et al*. 2018).

The results of the simulation are shown in the control chart of Fig. 17: the T^2 statistic suddenly increases since the simulated frequency shifts were applied (December 16th, 2020) and almost permanently trespass the UCL, even for very slight frequency drops.

7. Conclusions

The Main Spire of the Milan Cathedral is an iconic cultural heritage structure of the city of Milan, consisting of a slender octagonal structure in Candoglia marble supported by the main dome and the *tiburio* of the Cathedral. The monitoring system, recently installed in the Cathedral, includes seismometers (electro-dynamic velocity sensors) and temperature sensors at 3 levels of the Main Spire as well as a weather station at the top of the spire.

The paper describes the Structural Health Monitoring project of the Main Spire, comprising: (a) pre-processing and statistical analysis of the collected velocity signals; (b) continuous estimation of the modal parameters; (c) removal of the influence of environmental/operational factors through PCA and (d) novelty analysis to detect slight changes in the statistical properties of the identified natural frequencies.

Based on the results obtained in the first 16 months of continuous monitoring (i.e., from October 16th, 2018 to February 15th, 2020), the following main conclusions can be drawn:

- The monitoring system and the application of automated operational modal analysis allows the identification and tracking of 9 local modes of vibration of the spire in the frequency range 1-7 Hz;
- The evolution in time of the natural frequencies during the investigated period (16 months) of continuous monitoring reveals a distinctive correlation between resonant frequencies and temperature. In more details, all frequencies increase with decreased seasonal temperature and some of them (f_{S1}, f_{S2}, f_{S5} and f_{S6}) also exhibit a positive correlation with temperature on a daily basis, especially during the hot season;
- A couple of resonant frequencies (i.e., f_{S3} and f_{S4}) is also sensitive to the level of dynamic excitation associated with wind, with clear frequency drops occurring in correspondence to wind gusts;
- Beyond the peculiar effect exerted by environmental/ operational conditions on the natural frequencies, the correlation between frequencies is remarkably linear and suggests the adoption of PCA-based regression for the removal of the common trends of variation from the identified frequencies. The adopted PCA-based regression retains 4 principal components;
- The application of Hotelling's T^2 control charts to the frequency residuals in the investigated time span highlights that no significant structural changes occurred to the monumental structure. Furthermore, numerical simulations of slight damage scenarios confirmed the effectiveness of the adopted SHM procedure in detecting very slight frequency shifts.

Furthermore, it is worth mentioning that the information obtained from the continuous monitoring might be complemented by the development of a numerical (Finite Element) model of the Main Spire. Firstly, the dynamic characteristics of the spire should be used to address the main uncertainties of the model (i.e., related to the structural parameters characterizing the different parts of the historic building and to the interaction between the spire and the cathedral); subsequently, the model should be used to better understand the behavior of the spire and its response to changing environmental and operational conditions.

Acknowledgments

The support of *Veneranda Fabbrica del Duomo di Milano* is gratefully acknowledged. The authors would like to thank the technical staff of AGISCO and *Veneranda Fabbrica del Duomo di Milano* for the installation of all monitoring devices, and the technical staff of SARA Electronics Instruments for the assistance during the mounting and the initial operational setting of the seismometers.

References

Azzara, R.M., De Roeck, G., Girardi, M., Padovani, C., Pellegrini, D. and Reynders, E. (2018), "The influence of environmental parameters on the dynamic behaviour of the San Frediano bell tower in Lucca", *Eng. Struct*., **156**, 175-187. https://doi.org/10.1016/j.engstruct.2017.10.045

Cabboi, A. (2013), "Automatic operational modal analysis: challenges and application to historic structures and infrastructures", Ph.D. Thesis, University of Cagliari, Italy.

Cabboi, A., Magalhães, F., Gentile, C. and Cunha, À. (2017a), "Automated modal identification and tracking: application to an iron arch bridge", *Struct. Control Health Monitor*., **24**(1), e1854. https://doi.org/10.1002/stc.1854.

Cabboi, A., Gentile, C. and Saisi, A. (2017b), "From continuous vibration monitoring to FEM-based damage assessment: application on a stone-masonry tower", *Constr. Build. Mater*., **156**, 252-265. https://doi.org/10.1016/j.conbuildmat.2017.08.160

Cigada, A., Scaccabarozzi, M., Zappa, E. and Castiglione, B.M.V. (2020), "Critical measurement issues in the use of wire potentiometers for the structural health monitoring of slender structures: the case of the Duomo di Milano main spire", *J. Civil Struct. Health Monitor*., **10**(1), 119-134. https://doi.org/10.1007/s13349-019-00373-4

Deraemaeker, A., Reynders, E., De Roeck, G. and Kullaa, J. (2008), "Vibration-based structural health monitoring using output-only measurements under changing environment", *Mech. Syst. Signal Pr.*, **22**, 34-56. https://doi.org/10.1016/j.ymssp.2007.07.004

Diaferio, M., Foti, D. and Potenza, F. (2018), "Prediction of the fundamental frequencies and modal shapes of historic masonry towers by empirical equations based on experimental data", *Eng. Struct.*, **156**, 433-442. https://doi.org/10.1016/j.engstruct.2017.11.061

Elyamani, A., Caselles, O., Roca, P. and Clapes, J. (2017), "Dynamic investigation of a large historical cathedral", *Struct. Control Health.*, **24**(3), e1885. https://doi.org/10.1002/stc.1885

Ferrari da Passano, C. (1973), Storia della Veneranda Fabbrica del Duomo (in Italian), Cassa di Risparmio delle Province Lombarde, Milan, Italy.

Gentile, C., Guidobaldi, M. and Saisi, A. (2016), "One-year dynamic monitoring of a historic tower: damage detection under changing environment", *Meccanica*, **51**(11), 2873-2889. https://doi.org/10.1007/s11012-016-0482-3

Gentile, C., Ruccolo, A. and Canali, F. (2019), "Long-term monitoring for the condition-based structural maintenance of the Milan Cathedral", *Constr. Build. Mater.*, **228**, 117101. https://doi.org/10.1016/j.conbuildmat.2019.117101

Heylen, W., Lammens, S. and Sas, P. (2007), *Modal Analysis: Theory and Testing*, KU Leuven, Belgium.

Jolliffe, I.T. (2002), *Principal Component Analysis*, Springer, New York, USA.

Kita, A., Cavalagli, N. and Ubertini, F. (2019), "Temperature effects on static and dynamic behavior of Consoli Palace in Gubbio, Italy", *Mech. Syst. Signal Pr.*, **120**, 180-202. https://doi.org/10.1016/j.ymssp.2018.10.021

Magalhães, F. (2010), "Operational modal analysis for testing and monitoring of bridges and special structures", Ph.D. Thesis, Faculty of Engineering of the University of Porto, Portugal.

Masciotta, M.G., Roque, J.C.A., Ramos, L.F. and Lourenço, P.B. (2016), "A multidisciplinary approach to assess the health state of heritage structures: The case study of the church of Monastery of Jerónimos in Lisbon", *Constr. Build. Mater.*, **116**, 169-187. https://doi.org/10.1016/j.conbuildmat.2016.04.146

Masciotta, M.G., Ramos, L.F. and Lourenço, P.B. (2017), "The importance of structural monitoring as a diagnosis and control tool in the restoration process of heritage structures: A case study in Portugal", *J. Cultural Heritage*, **27**, 36-47. https://doi.org/10.1016/j.culher.2017.04.003

Montgomery, D.C. (1997), *Introduction to Statistical Quality Control*, John Wiley & Sons, New York, USA.

Nava, A. (1848), *Relazione dei ristauri intrapresi alla Gran Guglia del Duomo di Milano*, Tipografia Valentini & C, Milan, Italy. [In Italian]

Pappa, R.S., Elliott, K.B. and Schenk, A. (1992), A Consistent-mode indicator for the eigensystem realization algorithm, NASA Technical Memorandum 107607, NASA Langley Research Center, Hampton, USA.

Peeters, B. and De Roeck, G. (1999), "Reference-based stochastic subspace identification for output-only modal analysis", *Mech. Syst. Signal Pr.*, **13**(6), 855-878. https://doi.org/10.1006/mssp.1999.1249

Potenza, F., Federici, F., Lepidi, M., Gattulli, V., Graziosi, F. and Colarieti, A. (2015), "Long-term structural monitoring of the damaged Basilica S. Maria di Collemaggio through a low-cost wireless sensor network", *J. Civil Struct. Health Monitor.*, **5**(5), 655-676. https://doi.org/10.1007/s13349-015-0146-3

Reynders, E., Houbrechts, J. and De Roeck, G. (2012), "Fully automated (operational) modal analysis", *Mech. Syst. Signal Pr.*, **29**, 228-250, https://doi.org/10.1016/j.ymssp.2012.01.007

Roselli, I., Malena, M., Mongelli, M., Cavalagli, N., Gioffrè, M., De Canio, G. and de Felice, G. (2018), "Health assessment and ambient vibration testing of the Ponte delle Torri of Spoleto during the 2016–2017 Central Italy seismic sequence", *J. Civil Struct. Health Monitor.*, **8**(2), 199-216. https://doi.org/10.1007/s13349-018-0268-5

Ubertini, F., Cavalagli, N., Kita, A. and Comanducci, G. (2018), "Assessment of a monumental masonry bell-tower after 2016 Central Italy seismic sequence by long-term SHM", *B. Earthq. Eng.*, **16**(2), 775-801. https://doi.org/10.1007/s10518-017-0222-7

Veneranda Fabbrica del Duomo (1885), Annali della Fabbrica del Duomo di Milano: Dall'origine fino al presente (in Italian), Veneranda Fabbrica del Duomo, Milan, Italy.

Vicentini, G. (1906), Il pendolo registratore dei movimenti dell'aguglia maggiore del Duomo di Milano (in Italian), Hoepli, Milan, Italy.

Zacchi, A. (1941), "Private communication", *Archives of Veneranda Fabbrica del Duomo*, Milan, Italy. [In Italian]

Zonno, G., Aguilar, R., Borosheck, R. and Lourenço, P.B. (2019), "Analysis of the long and short-term effects of temperature and humidity on the structural properties of adobe buildings using continuous monitoring", *Eng. Struct.*, **196**, 109299. https://doi.org/10.1016/j.engstruct.2019.109299